

Local Track Reconstruction for the First Level Trigger in the CMS Muon Barrel Chambers

L. Castellani, M. De Giorgi, I. Lippi, R. Martinelli, A. J. Ponte Sancho¹, P. Zotto²
 INFN, Padova, Italy (email: Pierluigi.Zotto@padova.infn.it)

1) Now at Universidade do Algarve, UCEH, Gambelas, FARO, Portugal

2)Also at Dipartimento di Fisica, Politecnico di Milano, Milano, Italy

Abstract

The CMS muon chambers were designed to be a self-triggering device, using an algorithm which provides a rough track reconstruction like in the traditional Level-2 triggers. The track fitting dedicated ASIC devices were designed and have already been produced. A detailed description of their architecture and performance is given.

1. INTRODUCTION

The proposed CMS first level muon trigger primitive generator is a multistage scheme. The front-end trigger device is called Bunch and Track Identifier (BTI): it performs a rough track reconstruction and uniquely identifies the parent bunch crossing of the candidate track by means of a generalized mean-timer technique [1]. The device was realized and prototypes were recently tested.

The BTI is followed by a Track Correlator (TRACO) that is required to associate portions of tracks in the same chamber combining groups of BTIs among them. The TRACO enhances the angular resolution and produces a quality hierarchy of the triggers.

Its introduction is necessary since the BTI is intrinsically noisy and therefore a local preselection and a quality certification of the BTI triggers is required. The TRACO design is completed and submitted for prototype production.

TRACO trigger data are transmitted to the chamber Trigger Server (TS) [2]: the TS of the transverse view selects two tracks (looking for the lowest bending angle) among all tracks transmitted by the TRACOs; the TS of the longitudinal view sends the wired-or of the BTI trigger outputs to TRACOs for trigger qualification purposes and codes the triggers in a 32 bits string giving all the tracks pointing to the vertex with a position resolution of 8 cm.

The trigger information is transmitted to the Muon Regional Trigger using optical links.

2. DESCRIPTION OF BTI

The Bunch and Track Identifier was studied to work on groups of four layers of staggered drift tubes called Super Layers (SL). A muon barrel chamber is composed of two SL in the CMS transverse plane and one SL in the longitudinal one. Each SL is equipped with BTIs: thus we position and direction of tracks crossing any SL is measured. Each BTI is connected to nine wires allocated as shown in Figure. 1.

The parameters actually computed by the BTI are the angular k-parameter $k = h \tan \psi$ and the crossing position in the SL center. The geometrical quantities involved are shown in Figure 1: ψ is the angle of the track with respect to the normal to the chamber plane and $h = 1.3mm$ is the distance between the wire planes.

The BTI track finding algorithm computes in parallel several track patterns hypotheses: a pattern is identified from a sequence of wire numbers and labels stating if the track crosses the tube on the right or on the left of the given wire (e.g. in Figure 1 the track corresponds to the pattern 5L3R6L4R). Any given pattern includes six pairs of planes (AB, BC, CD, AC, BD, AD), each one providing a measurement of the position (through an *x-equation*) and of the k-parameter (through a *k-equation*) of the track. The definition and the full list of the preloaded patterns is available in [3].

The value of a *k-equation* is proportional to the sum or the difference of the hits arrival time of each pair of planes and corresponds to a rough measurement of the track direction. This value is generally time dependent. Each pair included in a pattern gives its own measurement of the track direction: the hits are aligned when, after applying a pair dependent proportional factor, the values of the k-parameter of each pair are equal.

Hence at every clock cycle all *k-equations* are computed and a BTI trigger is generated if at least three of the six k-parameters associated to any of the patterns are in coincidence. The tolerance on the coincidence of the *k-equations* is defined according to the resolution of each pair, that in turn depends on the distance between the wires and was chosen to allow a maximum cell linearity error equivalent to 25ns. This coincidence allows the bunch crossing identification owing to the time-dependence of the *k-equations* value.

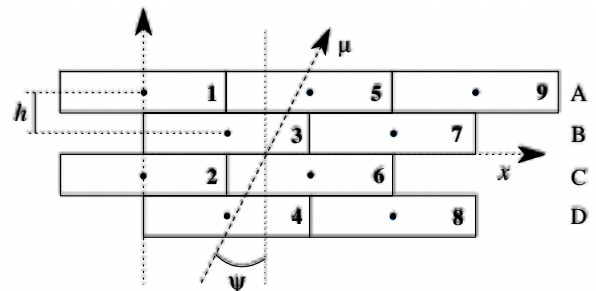


Figure 1 - Allocation of BTI input channels.

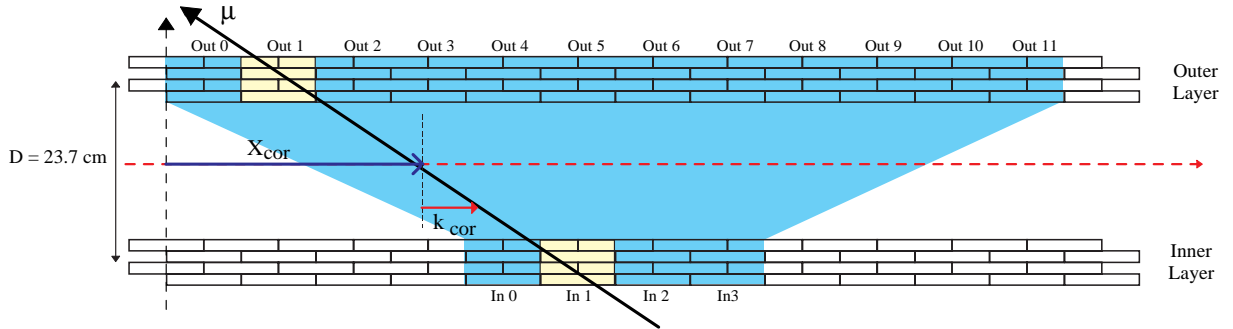


Figure 2 - TRACO layout.

If there is a coincidence of all the six k -parameters, the trigger corresponds to the alignment of four hits and it is marked as High Quality Trigger (HTRG), while in any other case, with a minimum of three coincident k -parameters, it is due to the alignment of only three hits and it is marked Low Quality Trigger (LTRG).

If several track patterns give a response, the HTRG is chosen as the triggering track pattern. If there is more than one HTRG or the triggers are all LTRGs, the first one, in an arbitrarily defined order, is selected.

The computed parameters, coded in 6 bits and accompanied by a TRG signal and a quality signal marking H or L, are transmitted with fixed delay with respect to the parent bunch crossing time, thus permitting its identification. The total latency of the BTI is determined by the maximum drift-time to the wires, T_{MAX} , plus 4 clock cycles needed for input signal synchronization and BTI calculations. For a nominal drift velocity of $50 \mu\text{m/ns}$ the delay of the TRG signal with respect to parent crossing is 20 bunch crossings.

Position and angular resolution of the device depend on the drift velocity and on the sampling frequency of the device. For a nominal drift velocity of $50 \mu\text{m/ns}$ and a sampling frequency of 80 MHz, the angle is measured with a resolution better than 60mrad , while the position is measured with a resolution of 1.25mm . The angular resolution of LTRGs is track pattern dependent and is generally worse than the one of HTRGs.

With the present geometric parameters of the chamber, the angular acceptance is nominally $\psi_{MAX} = \pm 45^\circ$, although the device works with reduced efficiency till 55° .

Each SL is equipped with one BTI every four wires and the BTIs are overlapped by five wires assuring that every track, with angle within the maximum acceptance range, is fully contained in at least one BTI.

Only one track per bunch crossing per BTI is forwarded to the TRACO.

3. TRACO DESCRIPTION

The TRACO is a processor that interconnects the two SL of the transverse plane. It receives the information from the BTIs connected to it and tries, linking the inner

layer triggers to the outer layer triggers, to find the pair of BTI track candidates that fits the best track.

The number of BTIs connected to a TRACO is pad-limited and it is determined by the acceptance requirement. The present design connects four BTIs of the inner SL to twelve BTIs of the outer SL allocated as shown in Figure 2, assuring a full coverage until ψ_{MAX} .

The algorithm starts selecting, among all the candidates in the inner SL and the outer SL independently, the best track segment, according to preferences given to the trigger quality (H/L) and to the proximity to the radial direction to the vertex (i.e. its p_T).

Then it computes the k -parameter and the position of a correlated track candidate. The compatibility between the k -parameters of the portions of track selected in the inner and outer SLs and the correlated track is checked against a programmable tolerance.

The internal parameters computed for the correlated tracks are:

$$\begin{cases} k_{COR} = \frac{D}{2} \tan \psi = x_{inner} - x_{outer} \\ x_{COR} = \frac{(x_{inner} + x_{outer})}{2} \end{cases}$$

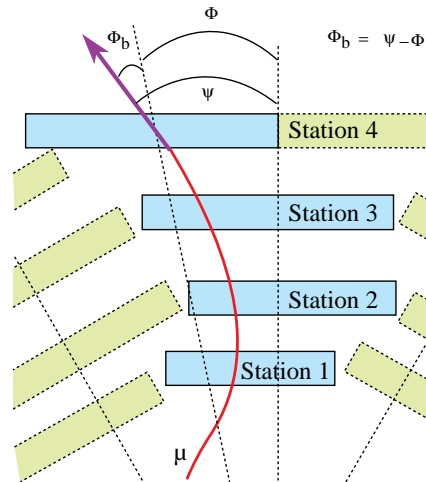


Figure 3 - Definition of TRACO output parameters.

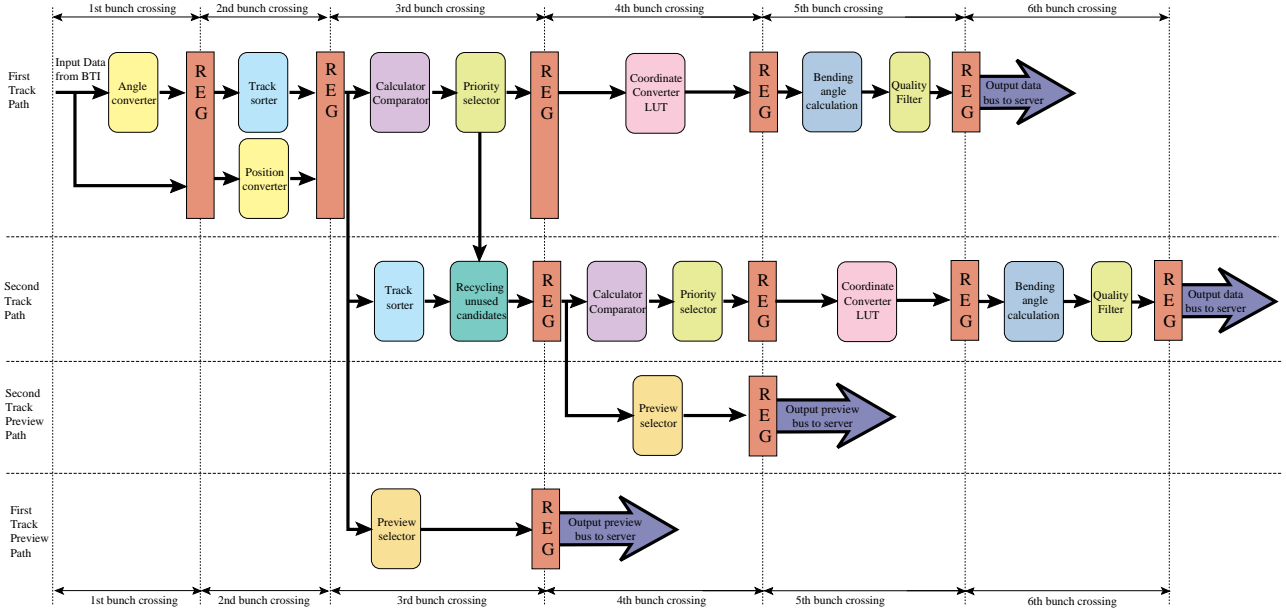


Figure 4 - Block description of TRACO operations.

The angular resolution of a correlated track candidate is 10mrad for the nominal drift velocity, thus improving the BTI value, while the resolution of the position remains unchanged.

These parameters are converted, using a programmable look-up table, to the chamber reference system: position is transformed to radial angle ϕ and k-parameter to bending angle ϕ_b as defined in Figure 3. The chosen track is forwarded to the chamber TS, for further selection.

If the correlation fails the correlator forwards an uncorrelated track following a preference list that includes the parent SL (IN/OUT) and the quality bit (H/L) of the two tracks selected for correlations.

If no correlation is possible since there is no candidate in one SL, the uncorrelated track is still forwarded.

The track is output on a bus, using 10 bits for the bending angle and 12 bits for the radial angle and it is accompanied by three quality bits identifying HH, HL, LL, H_i , H_o , L_i , L_o track candidates with obvious symbols meaning.

A further preference selection can be activated to connect the trigger generated in the transverse view to the triggers generated from the BTIs in the longitudinal view. In particular, since the noise generated from the BTI algorithm is of LTRG quality, a programmable coincidence between the two views is foreseen to certify the uncorrelated LTRGs.

In order to allow the identification of two muons inside the same correlator, the same algorithm is applied twice to the data received from the BTI. Therefore sometimes a second track is forwarded to the chamber TS. The programmability of the preferences for the choice of the First Track and the Second Track are completely independent, although we believe that the same criteria should apply.

A further selection is needed in the case that more than one TRACO inside a chamber give a trigger. The communication between the TRACOs and the chamber TS to allow this decision is done using a PREVIEW information, in order to minimize the time needed for calculations of the whole trigger chain. A copy (called PREVIEW) of one of the candidates chosen for correlation is sent to the TS according to the programmed H/L and IN/OUT selection flags, before starting any correlation calculation. The TS selection is based on the quality of the PREVIEW (given by the BTI resolution) of the various candidates.

The block scheme of the TRACO implementation, as previously described, is given in Figure 4. The TRACO calculations use 6 bunch crossings.

4. TRIGGER PERFORMANCE

The correlator algorithm was implemented in the standard CMS software including all the possible programming choices. Several studies using the full GEANT simulation of the detector were done to see the effect on noise reduction and trigger efficiencies according with the programming parameters in order to decide their default values.

4.1 Noise generation mechanisms

The design of the devices included in the trigger chain was done with the purpose of providing a robust and efficient system. Unfortunately the way to meet these requirements introduces a certain number of redundancies in the system causing a non negligible fraction of false or duplicated triggers.

The BTI trigger algorithm can actually work requiring only three layers of staggered tubes. The drawback of this kind of choice is the fact that an inefficiency or a bad

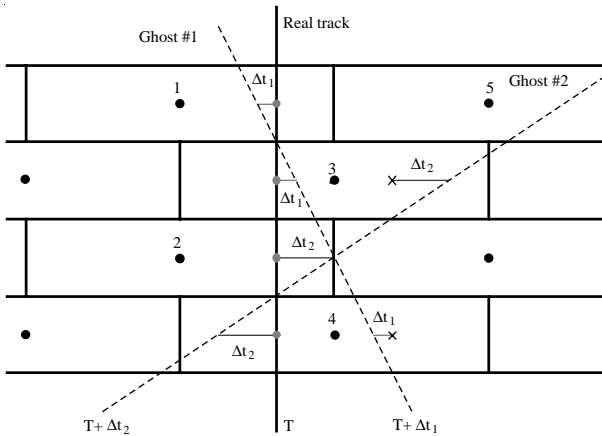


Figure 5 - Sketch of the generation mechanism of temporal noise inside the BTI.

measurement on any of the cells becomes an inefficiency or a wrong trigger. The introduction of the fourth layer with the minimal request of an alignment of three out of four hits enhances the efficiency and reduces the wrong measurements. But some spurious alignments of three hits can occur at any bunch crossing, depending on the track position and direction.

Most of the bad alignments are generated from the unavoidable left-right ambiguity even at several bunch crossing distance from the alignment of the four hits.

An example of the mechanism is shown in Figure 5, where a real track orthogonal to the chamber is displayed and the hit positions are marked with small circles on the track line. The BTI, looking for alignments of at least three hits, is able to find the alignment corresponding to the real track, but other two tracks are detected. These tracks, called *ghost tracks*, correspond to alignments of a mixture of real hits and their mirror images. In fact the BTI supposing that wire 2 is inefficient and that the signal of wire 4 comes from the right side of the tube, finds a false alignment at time Δt_1 after the right bunch crossing. In the same way, supposing that wire 5 is inefficient, the BTI finds another *ghost track*, formed from the signals of wires 2 and 4 and the mirror image of signal from wire 3, at time Δt_2 after the right bunch crossing.

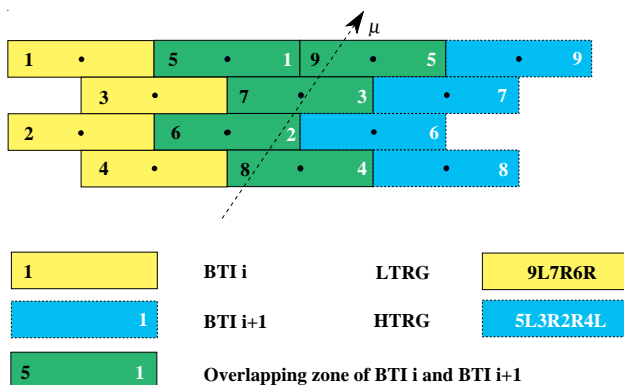


Figure 6 - Sketch of the spatial noise due to BTI overlap.

Let's call *noise of type I* the ghosts generated by this mechanism.

In order to be fully efficient the trigger system provides some overlap between adjacent devices: one BTI is overlapped by five cells to its neighbours and BTIs in the outer SL are always assigned to three consecutive TRACOs.

The overlap between BTIs is compulsory to obtain the needed angular acceptance. Furthermore it reduces the impact of the loss of one device on the trigger efficiency, since the remaining one can be programmed to at least partially cover the dead area switching on some redundant patterns.

Unlikely it is not possible to define a set of completely non-redundant patterns and therefore some of them are available in two consecutive BTIs: in fact there are five redundant patterns generating LTRGs on the devices close to the one generating the HTRG at the same bunch crossing.

In figure 6 we see a case where a valid HTRG pattern in one BTI is also seen as a valid LTRG pattern in the adjacent one.

Therefore the TRACO will have the chance to make a choice between candidate tracks in adjacent BTI's that are images of the same track, carrying exactly the same information. The First Track sorting will perform correctly, but it may result that the TRACO is forwarding

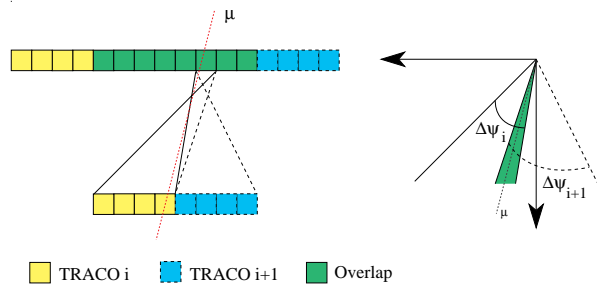


Figure 7 - Sketch of spatial noise due to TRACO overlap. The figure on the right reports at the same origin the angular acceptance of each TRACO on the left.

the same track twice, with a chance of losing other available candidates. This is called *noise of type II*.

The BTIs in the outer sorter are assigned to three consecutive TRACOs, being in the left, the central or the right group. This is another cause of noise generation (*noise of type III*). Since the TRACO is designed for a wide acceptance and must have some reasonable tolerance to be enough efficient, the candidate tracks can point to more than one TRACO as shown in Figure 7. Therefore, as in the case of adjacent BTIs, adjacent TRACOs can forward to the TS twice the same track. Again this fact may introduce a bias in the Second Track selection at the TS level where all TRACOs are put together.

4.2 Noise reduction methods

We have seen that there is a *temporal noise*, due to left-right ambiguity (*noise of type I*), that generates ghost tracks at wrong bunch crossings and *spatial noise* caused either by redundancy of the BTI equations (*noise of type II*) or by the overlap of the BTI acceptance ports (*noise of type III*), generating copies of the same track.

Some filters have been provided to reduce the overall importance of these effects in case the generated background will prove to be not tolerable once on site.

In order to reduce the *type I noise* we introduced a temporal Low Trigger Suppression: the low quality tracks (LL, L₀, L_i) are canceled if a HTRG occurred within the neighbouring bunch crossings. This suppression is applied at bunch crossings -1 to +8 with respect to any HTRG within the BTI, while it is also possible to suppress triggers at bunch crossings from -1 to -4 with respect to any HTRG inside the TRACO, without any latency addition.

Spatial noise can affect only the Second Track selection. It is possible to avoid sending twice the same track using a geometrical suppression filter. If a HTRG was selected in the First Track sorting operation, all the LTRG in the neighbouring BTIs are removed from the Second Track sorting list. This filter, always active, acts on *type II noise*. A similar procedure inhibiting Second Track LTRG selection can be applied to neighbouring TRACOs inside chamber TS to remove *type III noise*.

There is another possible cut to be applied to clean the TRACO output: a programmable tolerance window is implemented for the bending angle. This filter makes use of the fact that after traversing the coil any track will bend back, since it will find an opposite sign magnetic field. The bending angle as a function of momentum at all the muon stations is shown in Figure 8. Indeed there is a large spread for the average bending values at stations one and two, while it is close to zero at station three. Energy loss causes an overbending of low momentum muons at station four.

We cannot safely apply any cut in the first and second

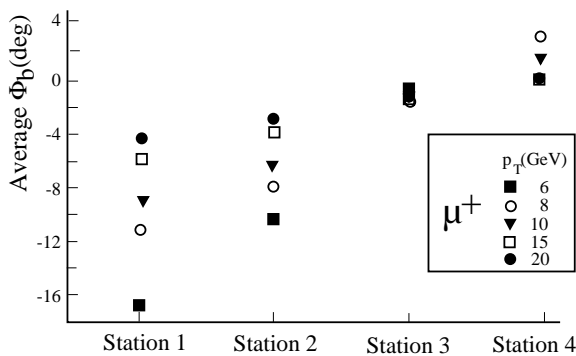


Figure 8 - Average value of the bending angle at the CMS four barrel muon stations for different muon p_T.

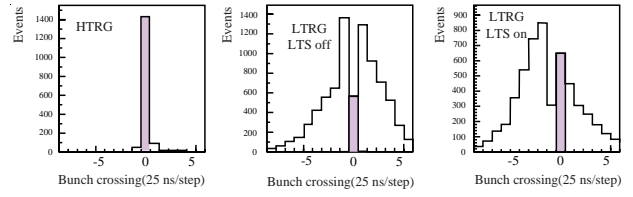


Figure 9 - Time distribution of BTI output triggers for different quality categories. The correct bunch crossing is shaded.

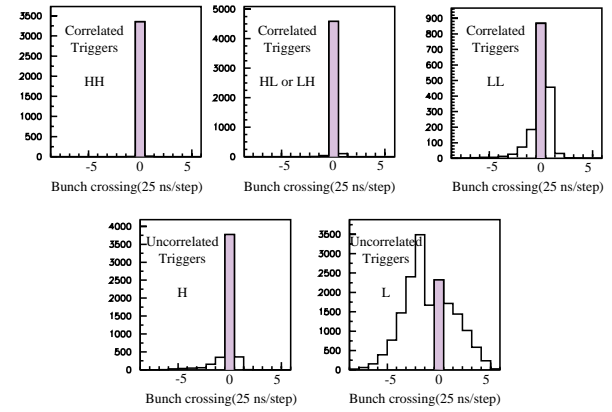


Figure 10 - Time distribution of TRACO output triggers for the different quality categories. The correct bunch crossing is shaded.

station, while an acceptance window on the bending angle can be used for station 3 and/or 4.

4.3 Efficiency studies

A large number of simulations was performed to check the trigger performance, The most interesting results are the ones concerning the temporal noise distribution and the trigger efficiency in various configurations.

Figure 9 shows the temporal distribution of HTRGs and LTRGs at the BTI output. While the HTRGs are a

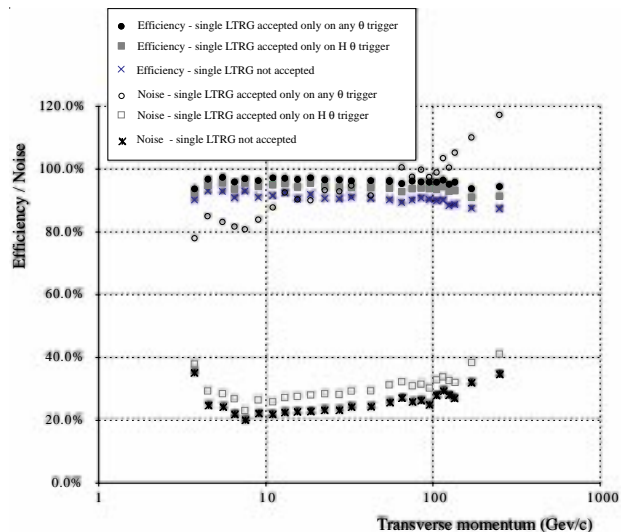


Figure 11 - Efficiency and noise for station 1 as a function of muon p_T for different trigger configurations.

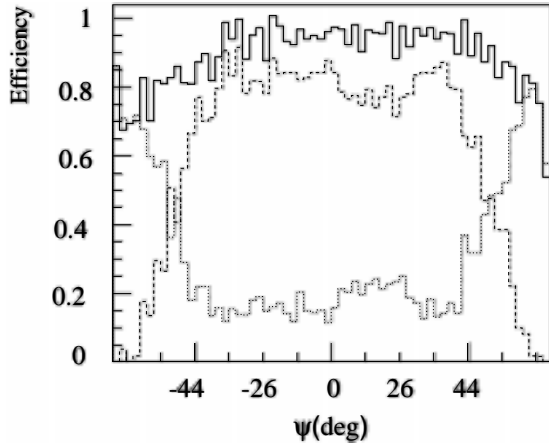


Figure 12 - TRACO efficiency versus the angle of incidence for all trigger (solid line), correlated tracks (dashed line) and uncorrelated tracks (dotted line).

clean signal we see that the LTRGs are distributed around the correct bunch crossing and therefore needs to be adequately certified.

Figure 10 shows the time distribution of the different categories of triggers output from the TRACO. Categories including at least one HTRG are again quite clean, while the other categories are badly identifying bunch crossing.

The single station efficiency, corrected for acceptance, of the trigger for few different choices of the noise reduction algorithms is reported in Figure 11. We conclude that we have means of reducing the noise with negligible efficiency loss.

Figure 12 shows the efficiency as a function of the angle of incidence for the relative fractions of correlated and uncorrelated tracks: the correlated triggers dominate till 45° as expected from TRACO acceptance design.

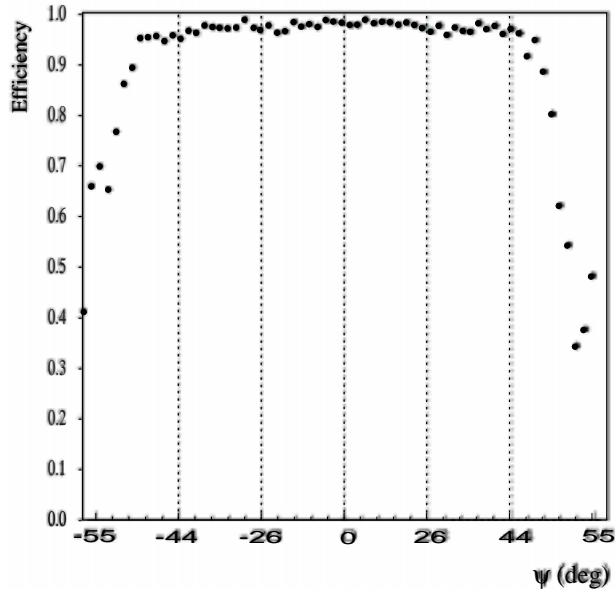


Figure 13 - Benchmark result of BTI efficiency versus the angle of incidence (Low Trigger Suppression off).

Table 1: Effect of bending angle cut on efficiency and noise at station 4

Φ_b cut	Efficiency	Noise
51.6	98.0%	102%
43.5	97.0%	83%
32.3	96.8%	72%
17.5	95.1%	56%
9.0	76.2%	34%

Table 1 shows the effect of the bending angle cut on efficiency and noise for $p_T = 8\text{GeV}/c$ tracks.

5. CURRENT STATUS

While the TRACO has been completely designed and submitted for a test production, a sample of BTIs was already produced, mounted on board, tested on bench and on a muon beam.

The benchmark was composed by a 40K sample of hits generated using the full GEANT simulation of single muons in front of a BTI in order to have a realistic spectrum of the input data.

The efficiency as a function of the angle of incidence is reported in Figure 13, showing that we have a flat response till 45° , while efficiency is rapidly falling till 55° , matching our design expectations.

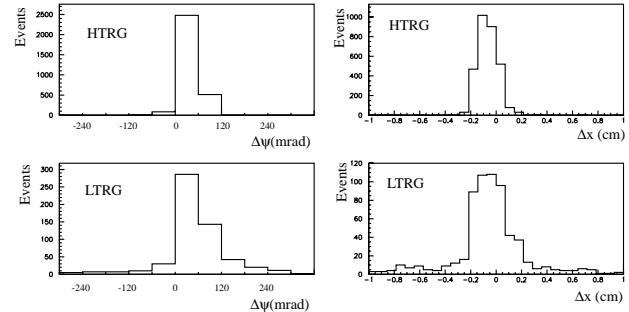


Figure 14 - Test beam result on angular and position resolution for different trigger quality categories of $80\text{ GeV}/c$ muons at normal incident angle.

The beam test was quite recent (end of August 1998), but apparently it was successful. As an example of the BTI performance in Figure 14 we show the angular and position resolution obtained for $80\text{ GeV}/c$ muons at normal incidence.

REFERENCES

- [1] F. Gasparini et al., Nucl Instr. and Meth. A336 (1993), 91.
- [2] A. Montanari, Track-Segment sorting in the Trigger Server of a Barrel Muon Station in CMS, these Proceedings.
- [3] M. De Giorgi et al., CMS TN/95-01 (1995)